

Adhesive cutaneous conducting polymer electrodes **F**

Cite as: Appl. Phys. Rev. **9**, 021401 (2022); <https://doi.org/10.1063/5.0079616>

Submitted: 23 November 2021 • Accepted: 15 March 2022 • Published Online: 01 April 2022

Published open access through an agreement with JISC Collections

 Ivan B. Dimov,  Armin Sautter, Wilfried Lövenich, et al.

COLLECTIONS

Paper published as part of the special topic on [Flexible and Smart Electronics](#)

F This paper was selected as Featured



View Online



Export Citation



CrossMark

ARTICLES YOU MAY BE INTERESTED IN

[Highly stable PEDOT:PSS electrochemical transistors](#)

Applied Physics Letters **120**, 073302 (2022); <https://doi.org/10.1063/5.0079011>

[Wireless, minimized, stretchable, and breathable electrocardiogram sensor system](#)

Applied Physics Reviews **9**, 011425 (2022); <https://doi.org/10.1063/5.0082863>

[Driving forces and molecular interactions in the self-assembly of block copolymers to form fiber-like micelles](#)

Applied Physics Reviews **9**, 021301 (2022); <https://doi.org/10.1063/5.0083099>



Applied Physics
Reviews

Read. Cite. Publish. Repeat.

19.162
2020 IMPACT FACTOR*



Adhesive cutaneous conducting polymer electrodes

Cite as: Appl. Phys. Rev. **9**, 021401 (2022); doi: [10.1063/5.0079616](https://doi.org/10.1063/5.0079616)

Submitted: 23 November 2021 · Accepted: 15 March 2022 ·

Published Online: 1 April 2022








View Online



Export Citation



CrossMark

Ivan B. Dimov,¹  Armin Sautter,²  Wilfried Lövenich,²  Christian Neumann,²  and George C. Malliaras^{1,a)} 

AFFILIATIONS

¹Electrical Engineering Division, Department of Engineering, Cambridge University, 9 JJ Thompson Ave., CB3 0FA Cambridge, United Kingdom

²Heraeus Deutschland GmbH & Co KG, Heraeusstrasse 12-14, 63450 Hanau, Germany

Note: This paper is part of the special collection on Flexible and Smart Electronics.

^{a)}Author to whom correspondence should be addressed: gm603@cam.ac.uk

ABSTRACT

Conducting polymers are widely used as electrode coatings in electrophysiology to lower impedance and achieve higher quality recordings and more efficient stimulation. Their availability as dispersions that can be processed directly from solution makes them particularly attractive for applications, where low cost and compatibility with mechanically flexible substrates are important. In this work, we demonstrate that poly(3,4-ethylenedioxythiophene)-based conducting polymer films can be made adhesive to skin and polyimide by adding acrylic ester copolymer microparticles to the solution. The resultant films remained highly conducting despite incorporating at most 2.5% conducting polymer. We show that adhesive cutaneous electrodes fabricated using these coatings show comparable performance to commercial electrodes in forearm electromyography.

© 2022 Author(s). All article content, except where otherwise noted, is licensed under a Creative Commons Attribution (CC BY) license (<http://creativecommons.org/licenses/by/4.0/>). <https://doi.org/10.1063/5.0079616>

I. INTRODUCTION

With the advancement of data-transfer speeds and miniaturization, wearable electronics has become an increasingly feasible means of outpatient monitoring and analysis of athletic performance.^{1–3} This would make technologies, such as Holter electrocardiography (ECG), electromyography (EMG), and electroencephalography (EEG), more frequently employed in the clinical practice. As such, significant effort is expended in developing novel cutaneous electrodes with improved electrical performance and wearability.^{4–9}

A common approach for improving the properties of cutaneous electrodes is the use of coatings made of conducting polymers such as poly(3,4-ethylenedioxythiophene) polystyrene sulfonate (PEDOT:PSS).¹⁰ This approach has shown improvements in contact impedance in a variety of electrophysiology applications.^{11–13} Such polymeric coatings offer many benefits—mild solution processing conditions, including spin coating,¹⁵ screen printing,¹⁴ and inkjet printing¹⁵ as well as compatibility with mechanically flexible substrates.^{16,17} The properties of these electrodes have been modified by surfactants and secondary solvents to optimize morphology,¹⁸ crosslinkers to improve stability in water,^{19,20} and ionic liquids to improve mechanical properties.^{21,22}

Recently, PEDOT:PSS has been blended with polyurethane and sorbitol to realize stretchable, adhesive conductive films.²³ These films

displayed good adhesion to skin and made effective electrodes for recording ECG and EMG signals. However, it is important to note that polyurethane products can potentially be skin irritants,^{24,25} providing an impetus to find additional adhesion chemistries. Here, we report PEDOT-based conducting polymer electrode coatings that contain acrylic ester copolymer microparticles. The addition of these microparticles renders the conducting films strongly adhesive to skin and plastic. Applying these coatings to Au films deposited on thin polyimide substrates allowed us to construct electrodes of comparable performance to commercially available ones. The resulting composites show good electrical conductivity and, when coated on Au films, they lower impedance in a manner that reflects increased electrode capacitance. We apply these electrodes to EMG measurements and show that they record high quality data. These materials pave the way for immediate improvements in diagnostics, prosthetic control, and athletic performance analysis.

II. RESULTS

A. Wettability and adhesion

Films were prepared from dispersions containing the conducting polymer PEDOT-S (see methods for synthesis details) and acrylic ester copolymer microparticles, corresponding to solids ratios of adhesive to

conducting polymer of 40:1, 60:1, and 90:1. Sliding droplet angle measurements shown in Figs. 1(a) and 1(b) reveal the surface of the films to be hydrophobic and exhibit a large water contact angle hysteresis ($>100^\circ$). This is characteristic of rough surfaces undergoing Wenzel wetting.²⁶ Similar results were obtained for PEDOT:PSS films with acrylic ester copolymer microparticles (Fig. S2). In contrast, pristine PEDOT:PSS (Clevios PH1000) films without the adhesive microparticles are hydrophilic and show low contact angle hysteresis [Figs. 1(a) and 1(b)]. The hydrophobicity endowed by the addition of the acrylic ester copolymer microparticles is beneficial for adhesion, especially to hydrophobic surfaces, such as skin²⁷ and plastics. While adhesion to the skin is a necessity in cutaneous electrode applications, adhesion to plastics and industrial polymers is also beneficial, as it facilitates deposition without the use of crosslinkers such as GOPS or DVS.^{19,20,28}

As a test for adhesion, 20 μl droplets of the PEDOT-S composites were cast onto plasma cleaned Kapton films, annealed at 110 $^\circ\text{C}$ for 5 min, and immersed in water for a week. All the films survived the immersion and remained in place [Fig. 1(c)]. Films of PEDOT:PSS composites gave similar results (Fig. S1). The good stability in water is likely due to a strong interaction between the film and the Kapton substrate, both of which are hydrophobic. As a control, pristine PEDOT:PSS films deposited and annealed in the same fashion were found to delaminate after a few minutes of immersion [Fig. 1(c)], in agreement with previously reported results.²⁹

Finally, we performed peel tests of films deposited on Kapton and adhered to a steel plate to quantify adhesion [Figs. 1(d) and 1(e)]. The trend in adhesive force followed particle loading (0.071 ± 0.0097 , 0.082 ± 0.0056 , and 0.088 ± 0.0057 N, for 40:1, 60:1, and 90:1, respectively). Samples with lower particle ratios (20:1) did not display

measurable adhesion. The measured forces are in the range of those previously reported for adhesive electrodes,⁹ and comparable to the values for specialized preterm neonatal medical tape.³⁰

B. Electrical and electrochemical properties

Sheet resistance measurements were conducted on wire-bar coated films, revealing high conductivity for all PEDOT-S composites. The measured values were in the range of 2.5–10 $\text{k}\Omega \text{sq}^{-1}$ for 40 μm wet films and in the range of 30–80 $\text{k}\Omega \text{sq}^{-1}$ for 12 μm films [Fig. 2(a)]. PEDOT:PSS composites showed sheet resistance values that were significantly higher, but decreased to values of single $\text{k}\Omega \text{sq}^{-1}$ upon the addition of ethylene glycol in the dispersion (see Table S1). The addition of ethylene glycol did not reduce PEDOT-S sheet resistance (4.0 ± 0.6 , 7.0 ± 1.0 , and $27 \pm 4 \text{ k}\Omega \text{sq}^{-1}$ for 40 μm wet films at 40:1, 60:1, and 90:1 adhesive/PEDOT-S ratios). This is likely due to the structural difference between the materials—PEDOT:PSS is a blend of the two polymers, while PEDOT-S has covalently bound sulfonate groups to the PEDOT backbone. Ethylene glycol treatment typically induces structural reorganization in PEDOT:PSS.¹⁸

Electrochemical impedance spectroscopy (EIS) measurements were conducted in a custom-built electrochemical cell [Fig. 2(b)] that clamped the films to minimize substrate deformation. While not directly transferable to cutaneous applications, solution-phase EIS in buffer offers a physico-chemically defined system, allowing for fewer confounding variables (e.g., intrinsic biological variability between different volunteers and measurement sessions on the skin) when comparing formulations. The results, displayed in Fig. 2(c), show that PEDOT-S composites improve the impedance of Au electrodes at low

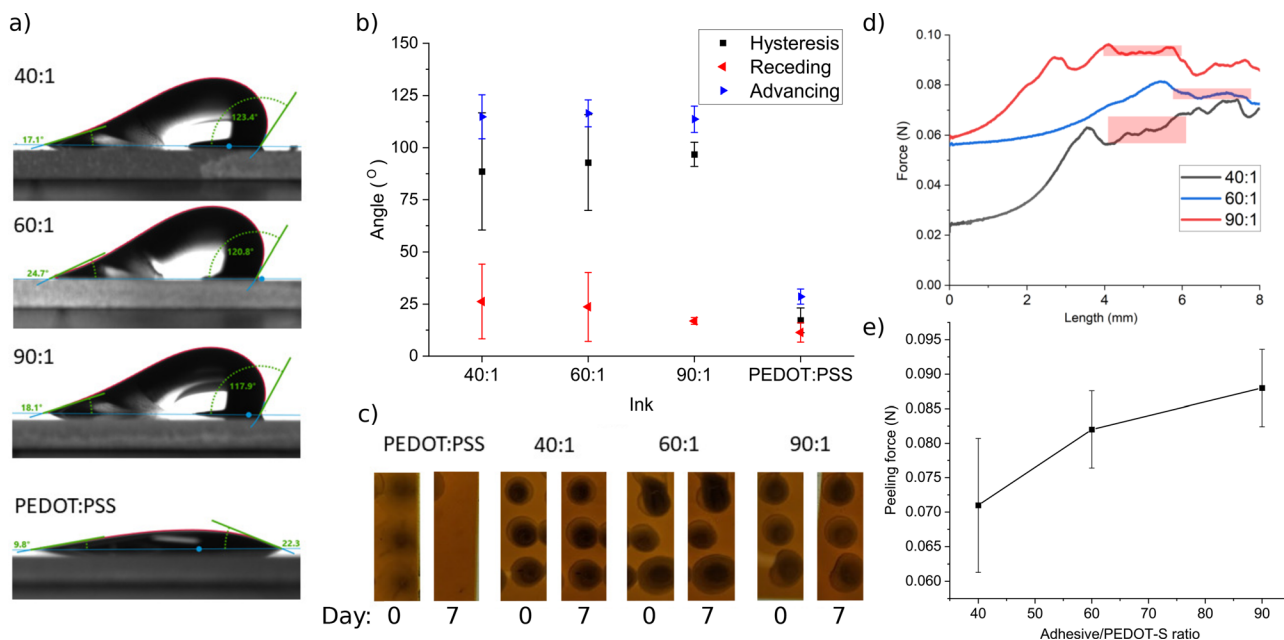


FIG. 1. (a) Representative images of droplets at maximum stage tilt for the different films. Sliding droplet angle measurements results. (b) Sliding droplet angle measurements results. (c) Photographs of films made by casting 20 μl droplets from the different composites, immediately after immersion and after 7 days in DI water. Pristine PEDOT:PSS was used as a control. (d) Representative peel tests from each film. Highlighted areas were averaged out to derive a value for each replicate. (e) Mean peeling force for different films.

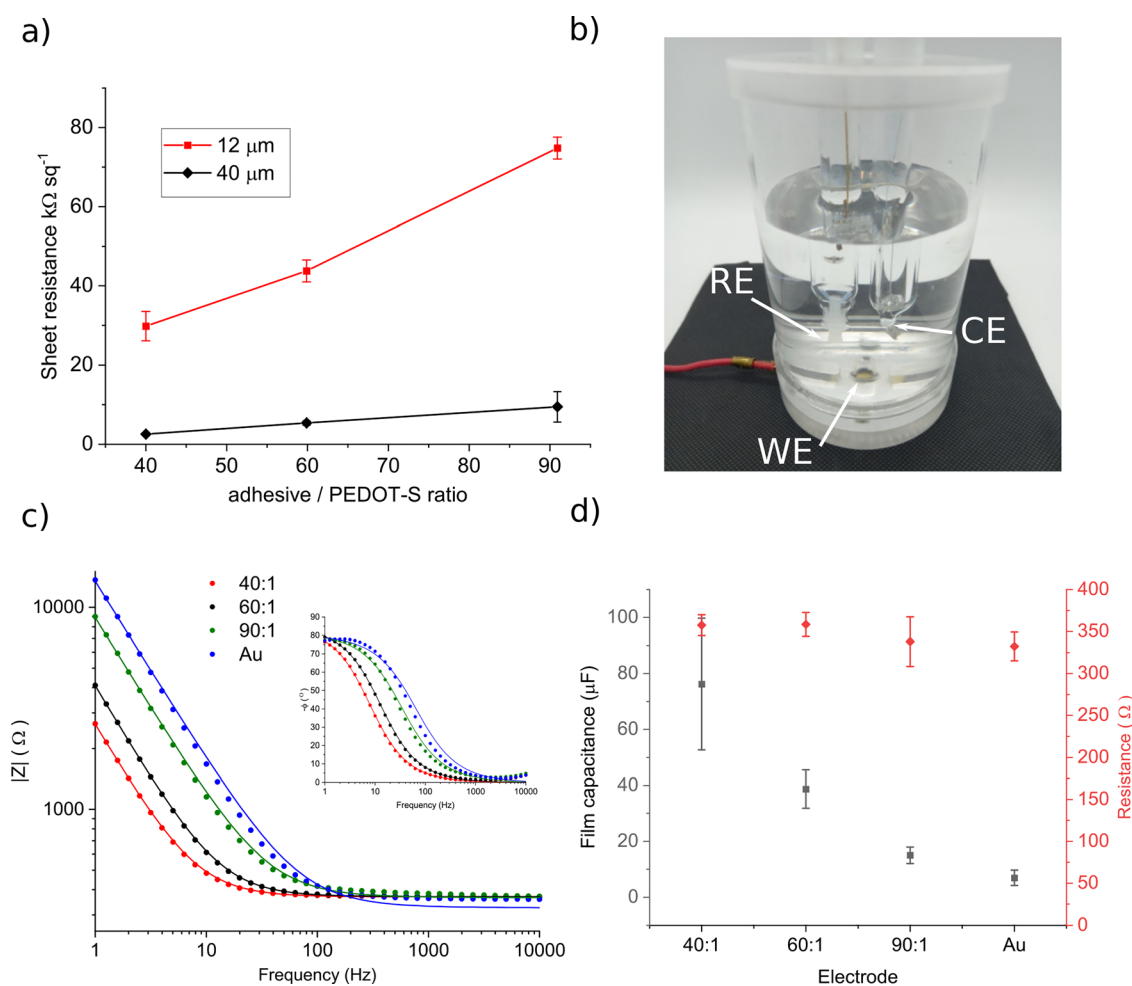


FIG. 2. (a) Sheet resistance data for adhesive/PEDOT-S blend, at two different wet-film thicknesses. Increasing thickness and lowering adhesive content lowers sheet resistance. (b) The setup for solution-phase EIS measurements, consisting of a small cylindrical tank, capable of clamping a thin-film sample, with mounting points for electrodes. WE—working, RE—reference, and CE—counter electrodes. (c) Representative EIS curves for impedance magnitude for each material. Inset shows phase angle. (d) Film capacitance and resistance from fitting the above data to an R-CPE model.

frequencies. This is consistent with previous measurements on conducting polymer film coatings, which attribute the impedance lowering to an increase in electrode capacitance due to volumetric ion transport in the polymer.¹³ Accordingly, the shape of the impedance spectra approximately corresponds to an equivalent circuit of a capacitor C (representing the polymer) in series with a resistor R (representing the electrolyte). Small deviations are observed from an ideal RC behavior, in terms of slightly lower phase angle, than the anticipated 90° at low frequencies. This is a common observation in inhomogeneous surfaces, such as the PEDOT derivatives/particulate blends studied here.³¹ Values for R and C , obtained by fits to the impedance data, are shown in Fig. 2(d). Values for resistance remain constant across the different electrodes, as expected by the fact that R is determined by the electrolyte. On the other hand, the capacitance of the composites changes in a systematic fashion, decreasing with adhesive particle loading. This is expected, as volumetric capacitance scales with the density of doping sites in the film.³² Taking into account film thickness as

measured by profilometry (1.1 ± 0.4 , 1.9 ± 0.2 , and $1.6 \pm 0.5 \mu\text{m}$ for the 40:1, 60:1, and 90:1 composites, respectively), we estimate volumetric capacitance of these films to be 2.4 ± 0.4 , 0.7 ± 0.1 , and $0.4 \pm 0.3 \text{ F cm}^{-3}$ for the 40:1, 60:1, and 90:1 composites, respectively. Extrapolating linearly to a pristine PEDOT-S film (i.e., no adhesive particles) gives a volumetric capacitance of $140 \pm 60 \text{ F cm}^{-3}$. This is significantly higher than the literature reported value of 39 F cm^{-3} for PEDOT:PSS, which can be attributed to the higher density of doping sites in PEDOT-S.³² In addition, the value carries a comparatively large error, potentially as we are extrapolating over a very large composition range. PEDOT:PSS composites showed complex impedance spectra, that could not be described with a simple RC equivalent circuit model (Fig. S3). The addition of ethylene glycol, on the other hand, changed the impedance spectra dramatically, allowing R and C values to be extracted (shown in Fig. S4). As expected, R is similar to that obtained for the PEDOT-S composites and the Au electrode, while C decreases with the increasing content of adhesive particles.

C. Recording of cutaneous biopotentials

Given that the PEDOT-S composites do not require the addition of ethylene glycol to give good impedance spectra, we proceeded with these materials for further characterization. EIS measurements were conducted on the arm of a volunteer, using a three-electrode configuration on the forearm with commercial electrodes used as a reference and counter [Fig. 3(a)].

PEDOT-S composite-coated films remained attached to the skin entirely by their own adhesive strength, without the use of any adhesive tape or external pressure. For plain gold films, contact was maintained by gently manually pressing the electrode against the skin. These experiments were conducted under approval from the Ethics Committee of the Department of Engineering. The data displayed in Fig. 3(b) show that the PEDOT-S composites form contacts of lower impedance to the skin than pristine Au electrodes. Slightly lower impedance is seen for the film with a 40:1 adhesive to PEDOT-S ratio, consistent with the film's higher conducting component loading.

We then proceeded to record EMG data from the palmar flexion of a volunteer, in a two-electrode setup, using the electrodes under test (a PEDOT-based and a commercial one) on the forearm, referenced to a commercial electrode on the elbow. This allowed us to estimate the signal-to-noise ratio (SNR) and compare it with that of a commercial electrode [Fig. 3(d)] of similar area (approximately 3 cm^2 for the PEDOT-based electrodes and 3.46 cm^2 for the commercial electrodes used). Differences between the three PEDOT-S composite electrodes

were comparatively small and not significant. This is consistent with the small observed differences in cutaneous impedance observed. This is likely due to cutaneous impedance being a quantity dependent on the quality of adhesion, on the electrochemical properties of the electrode, and on the state of the subject's skin between measurement sessions. Importantly, the commercial electrode performed with similar SNR (6.5 ± 2.9 , 7.5 ± 2.9 , 7.3 ± 3.4 , and 5.7 ± 2.3 , respectively, for 40:1, 60:1, 90:1, and the commercial electrode).

To explore whether the measured SNR is sufficient to extract meaningful signals, EMG data were recorded while the volunteer squeezed a grip-tester device, with different strengths. Due to the small observed difference in cutaneous impedance between the three formulations, we performed the measurements with the 40:1 blend. We observed increases in voltage amplitude clearly correlating with grip strength, indicating that the SNR is adequate for this type of application [Fig. 3(e)].

III. DISCUSSION

The composites showed higher conductivity and lower impedance with increasing conducting polymer fraction. A notable result is that good performance, in terms of conductivity, impedance, and SNR in EMG measurements, was achievable despite the low overall doping with conducting polymer. This would imply that a percolating conducting network is present even at the highest loading with adhesive particles (90:1). We speculate that this is due to complete separation between the two phases conducting polymer and adhesive particles,

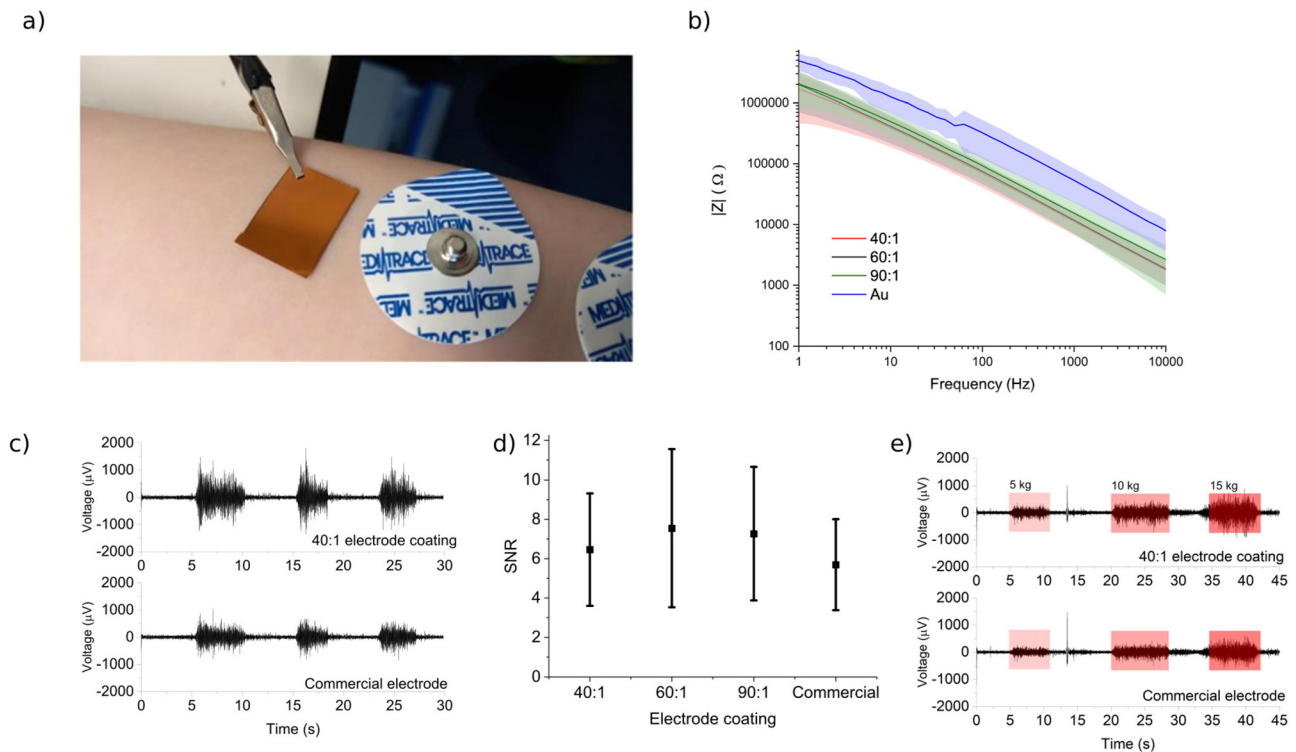


FIG. 3. (a) A photograph of a cutaneous EIS measurement experiment. The setup for EMG experiments was analogous, but featured one commercial electrode. (b) Average impedance magnitude over a range of frequencies, with the shaded areas displaying standard deviation ($n = 3$ per curve). (c) Representative trace of palmar flexion EMG recordings to establish maximum SNR. (d) SNR for various electrodes. (e) Representative recording of squeezing force gauge.

allowing a continuous conducting network to form. Interestingly, this occurs significantly below the typical range of percolation thresholds for conductor/dielectric mixtures.^{33–35} Both PEDOT-S and PEDOT:PSS could be rendered adhesive with the addition of acrylic ester copolymer microparticles, demonstrating the generality of this approach. PEDOT-S composites showed better performance (lower sheet resistance and well-behaved impedance spectra), while the addition of ethylene glycol in the PEDOT:PSS composites improved performance. We speculate that this is due to the more complex morphology of PEDOT:PSS, which is known to form films with two distinct (PEDOT-rich and PSS-rich) phases. In both composites, the addition of crosslinkers such as GOPS or DVS was not necessary to endow good film stability in water. This simplifies materials handling and processing, as cross-linking and hydrolysis reactions begin as soon as the crosslinker is added to the solution. In contrast, the acrylic ester copolymer microparticle containing dispersions are usable with no apparent alteration in properties for over a year.

IV. CONCLUSIONS

In this paper, we demonstrated that the addition of acrylic ester copolymer microparticles is a flexible approach that can improve the adhesive properties of conducting polymer electrodes. Using this approach, we successfully fabricated wearable electrodes with comparable electrical performance to commercially available ones. Segregation of the conducting polymer and adhesive microparticles seems to be the reason why high conductivity and low impedance are achieved even at high adhesive loadings.

V. MATERIALS AND METHODS

A. Materials

Unless otherwise indicated, reagents were purchased from Sigma-Aldrich. PEDOT:PSS and PEDOT-S dispersions are available from Heraeus Deutschland GmbH under the name RD Clevis F GL.

B. Conducting adhesive ink preparation

The conducting adhesive inks were prepared by blending different ratios of highly conducting aqueous PEDOT-S dispersions, adjusted to a pH of 5 with 0.1 N NaOH solution, with an aqueous acrylic ester copolymer adhesive dispersion. The microparticles are a commercial acrylic ester copolymer dispersion in water (ALRBERDINGK). The final formulations of microparticles and conductive polymer are available from Heraeus. PEDOT-S was prepared by polymerization of sodium 4-[(2,3-dihydrothieno[3,4-b][1,4]dioxin-2-yl)methoxy]butane-2-sulfonate (Na-EDOT-S) according to literature.³⁶ PEDOT-S had a specific conductivity σ of 250 S cm^{-1} . The aqueous acrylic ester copolymer adhesive dispersion had a solid content of 68% and a T_g of -46°C .³⁷ The solid content of the PEDOT-S and PEDOT:PSS inks used was 1.1 wt. %. The total solid content of all conducting adhesive inks was adjusted to 20 wt. % by dilution with de-ionized water in order to be able to coat of similar layer thicknesses. The calculated solids ratios of adhesive to conducting polymer are 40:1, 60:1, and 90:1. The conducting adhesive inks were coated with a wetfilm thickness of $12 \mu\text{m}$ and $40 \mu\text{m}$ by wirebar on a PET film (Melinex 506) and dried in a convection oven at 120°C for 5 min. The sheet resistances were measured with an ACL 800 Digital Megohmmeter (ACL Staticide). The tackiness of all dried conducting adhesive layers is strong and increases with the increasing ratio of adhesive to conducting polymer.

C. Water contact angle measurement

Glass slides were cleaned with DI water, acetone, and IPA and oxygen plasma treated. Inks were spin-coated on top (500 rpm for 5 s, followed by 1000 rpm for 30 s). Samples were then thermally annealed on a hot-plate at 110° for 5 min. Using a contact-angle goniometer (KRÜSS Scientific), $50 \mu\text{l}$ droplets were deposited, at $2 \mu\text{l/s}$. The stage was then tilted at $1^\circ/\text{s}$, up to 90° . Droplet profiles were fitted by the built-in tangent method on the KRÜSS Advance software. Advancing and receding contact angles were determined from the fits and used to calculate the contact angle hysteresis. Average values were reported.

D. Peel testing

A thin ($50 \mu\text{m}$) $2.5 \times 7.5 \text{ cm}^2$ Kapton film was cut out, cleaned with DI water, acetone, and IPA as above, plasma treated, and spin coated with ink. Subsequently, the films were thermally annealed as above. The films were then used for peel tests on a steel plate, using a 25 N load cell (Tinius Olsen), at a 10 mm/min loading rate. A 2 cm region from each peel curve was averaged and taken as the individual measurement result.

E. Electrode fabrication

A thin $5 \times 5 \text{ cm}^2$ Kapton film was rinsed with de-ionized water, acetone, and IPA. Afterward films were oxygen plasma treated at full power for 1 min, and a 5 nm Ti/100 nm Au stack was deposited on top, using electron beam evaporation. Subsequently, the resulting stack was laser-cut into pieces, $15 \times 20 \text{ mm}^2$, with rounded corners (1 mm radius). The stacks were oxygen-plasma treated and then spin-coated with ink formulations under investigation (5 s at 300 rpm, followed by 30 s at 1000 rpm), on a vacuum-free spin coater (Ossila, UK). Samples were then thermally annealed on a hot-plate at 110° for 5 min.

F. Electrochemical characterization

Electrochemical impedance spectroscopy was carried out on the samples, using a standard three-electrode setup, using an Ag/AgCl reference electrode (Metrohm AG, NL) and a platinum counter electrode (Metrohm AG, NL), in a standard phosphate buffered saline solution. A custom-made electrochemical cell, that could reproducibly clamp the sample using magnets, was used for the measurements. The electrochemically accessible area of each clamped film was a 6 mm diameter circle. The amplitude was 10 mV, and there was no DC bias with respect to the reference electrode. Scan range was from 1 to 10^4 Hz, unless otherwise indicated. Fits were performed with the impedance.py package,³⁸ by fitting a resistor in series with a constant-phase element, and a capacitance was extracted via the equation of Brug *et al.*³⁹ EIS measurements on the skin were carried out on the forearm, with commercial cutaneous electrodes as counter and reference (Medtrace ECG electrodes). Electrodes were positioned in order reference-counter-working from elbow to wrist, at approximately 1.5 cm edge-to-edge distance between them. All cutaneous EIS measurements were performed with the approval of the Ethics Committee of the Department of Engineering at the University of Cambridge (6/9/2018, IONBIKE) and after obtaining informed consent from volunteers.

G. Electrophysiological recording

All experiments were performed with the approval of the Ethics Committee of the Department of Engineering at the University of Cambridge (6/9/2018, IONBIKE) and after obtaining informed consent from volunteers. Electrophysiological recordings were carried out on an Intan RHS-1000 system. Commercial electrodes were held by a button adapter. Thin-film electrodes under investigation were attached to the same holder using a button electrode-to-alligator clip adapter. The alligator clip was insulated on the outside, to minimize contact with the skin. For forearm EMG measurements, the electrodes under test were placed on the left anterior forearm, referenced to a commercial electrode attached on the elbow (Red dot Multi-Purpose electrodes 2560, 3M). Recordings were carried out during 90° palmar flexion of the hand (i.e., palm toward forearm), with extended digits or while squeezing a grip-strength tester with a digital display. A metal alligator clip was attached to the tip of the elbow to act as a ground electrode. The recording was done at a 30 kHz sampling rate, with a 50 Hz notch filter. A software filter of 10–500 Hz was applied to the data, prior to analysis. To assess quantitatively the SNR, 30 s intervals were recorded, and within each interval, the subject's wrist was flexed three times, at 90° for 3–5 s at a time. From each trace, three 1-second intervals of the extended wrist were taken (noise intervals), and three 1-second intervals of different individual instances of wrist flexion were taken (signal intervals). The signal intervals were taken approximately 0.5 s after the onset of flexion, to avoid any mechanical noise from cable motion. The standard deviations (SD) of the recorded voltage during each interval were recorded. Subsequently, for every trace, the SD of the noise intervals were averaged, as were the signal interval SDs. Finally, the ratio of the average SD for the signal to noise is the reported value for each experiment. For all the PEDOT-S electrodes, three traces from three electrodes from different batches were taken. One trace for each electrode was taken from three different control electrodes were taken for the commercial control SNR.

SUPPLEMENTARY MATERIAL

See the [supplementary material](#) for details of the composition (S1), contact angle (S2), and solution-phase EIS data (S3 and S4) on PEDOT:PSS-based inks.

ACKNOWLEDGMENTS

This work was partially funded by Heraeus Deutschland GmbH Co and by the EPSRC (Pneumacrit, EP/T004908/1). The authors would like to acknowledge the assistance of Mr. Andrew Rayment in performing the peeling experiments.

AUTHOR DECLARATIONS

Conflict of Interest

The authors have no conflicts to disclose.

DATA AVAILABILITY

The data that support the findings of this study are available from the corresponding author upon reasonable request.

REFERENCES

- ¹E. Gibney, *Nature* **528**, 26 (2015).
- ²J. Rogers, G. Malliaras, and T. Someya, *Sci. Adv.* **4**, aav1889 (2018).
- ³C. Xu, Y. Yang, and W. Gao, *Matter* **2**, 1414 (2020).
- ⁴S. Choi, H. Lee, R. Ghaffari, T. Hyeon, and D. H. Kim, *Adv. Mater.* **28**, 4203 (2016).
- ⁵S. Choi *et al.*, *Nat. Nanotechnol.* **13**, 1048 (2018).
- ⁶W. Guo *et al.*, *ACS Appl. Mater. Interfaces* **11**, 8567 (2019).
- ⁷Z. Jiang *et al.*, *Adv. Mater.* **31**, 1904956 (2019).
- ⁸Y. Wang *et al.*, *Sci. Adv.* **6**, eabb9083 (2020).
- ⁹H. Wu *et al.*, *Adv. Sci.* **8**, 2001938 (2021).
- ¹⁰A. Elschner, S. Kirchmeyer, W. Lovenich, U. Merker, and K. Reuter, *PEDOT: Principles and Applications of An Intrinsically Conductive Polymer* (CRC Press, 2010).
- ¹¹P. Leleux *et al.*, *Adv. Healthcare Mater.* **3**, 1377 (2014).
- ¹²D. Khodagholy *et al.*, *Nat. Neurosci.* **18**, 310 (2015).
- ¹³D. A. Koutsouras *et al.*, *ChemElectroChem* **4**, 2321 (2017).
- ¹⁴S. K. Sinha *et al.*, *ACS Appl. Mater. Interfaces* **9**, 37524 (2017).
- ¹⁵E. Bihar *et al.*, *Adv. Healthcare Mater.* **6**, 1601167 (2017).
- ¹⁶S. Velasco-Bosom *et al.*, *Adv. Healthcare Mater.* **10**, 2100374 (2021).
- ¹⁷E. Bihar *et al.*, *Adv. Mater. Technol.* **2**, 1600251 (2017).
- ¹⁸J. Rivnay *et al.*, *Nat. Commun.* **7**, 11287 (2016).
- ¹⁹A. Håkansson *et al.*, *J. Polym. Sci., Part B* **55**, 814 (2017).
- ²⁰D. Mantione *et al.*, *ACS Appl. Mater. Interfaces* **9**, 18254 (2017).
- ²¹P. Leleux *et al.*, *Adv. Healthcare Mater.* **3**, 490 (2014).
- ²²M. Y. Teo *et al.*, *ACS Appl. Mater. Interfaces* **9**, 819 (2017).
- ²³L. Zhang *et al.*, *Nat. Commun.* **11**, 6013 (2020).
- ²⁴T. Estander, H. Keskinen, R. Jolanki, and L. Kanerva, *Contact Dermatitis* **27**, 161 (1992).
- ²⁵N. M. Lamba, K. A. Woodhouse, and S. L. Cooper, *Polyurethanes in Biomedical Applications* (Routledge, 2017).
- ²⁶G. McHale, *Langmuir* **23**, 8200 (2007).
- ²⁷M. E. Ginn, C. M. Noyes, and E. Jungermann, *J. Colloid Interface Sci.* **26**, 146 (1968).
- ²⁸I. del Agua *et al.*, *Adv. Mater. Technol.* **3**, 1700322 (2018).
- ²⁹S. Zhang *et al.*, *J. Mater. Chem. C* **4**, 1382 (2016).
- ³⁰B. Laulicht, R. Langer, and J. M. Karp, *Proc. Natl. Acad. Sci. U. S. A.* **109**, 18803 (2012).
- ³¹M. E. Orazem *et al.*, *J. Electrochem. Soc.* **160**, C215 (2013).
- ³²C. M. Proctor, J. Rivnay, and G. G. Malliaras, *J. Polym. Sci., Part B* **54**, 1433 (2016).
- ³³D. J. Kang, H. Kang, K.-H. Kim, and B. J. Kim, *ACS Nano* **6**, 7902 (2012).
- ³⁴I. Jerkovic, V. Koncar, and A. M. Grancaric, *Sensors* **17**, 2297 (2017).
- ³⁵R. M. Ziff and S. Torquato, *J. Phys. A* **50**, 085001 (2017).
- ³⁶A. Scheel, K. Asteman, M. Intelmann, and U. Merker, "Process for producing functionalized polythiophenes," WO2016102129 (2016).
- ³⁷C. Neumann, A. Sautter, and T. Asmus, "Self-adhesive electrode patch," WO2019020571 (2019).
- ³⁸M. D. Murbach, B. Gerwe, N. Dawson-Elli, and L.-K. Tsui, *J. Open Source Software* **5**, 2349 (2020).
- ³⁹G. J. Brug, A. L. van den Eeden, M. Sluyters-Rehbach, and J. H. Sluyters, *J. Electroanal. Chem. Interfacial Electrochem.* **176**, 275 (1984).